

Chapter 1

Bridging Materials and Pressure Gaps in Surface Science and Heterogeneous Catalysis

Jeong Young Park and Gabor A. Somorjai

1.1 Introduction

Over the last several decades, surface science has undergone revolutionary advances that reveal the atomic- and molecular-level structural, dynamic, compositional, and thermodynamic properties of surfaces that are utilized in chemical process development. Adsorption and reaction rates and catalytic selectivity are also better understood, making the design of surfaces that deliver desired chemical properties possible. In this book, we highlight recent works in surface science and catalysis with an emphasis on the development of new catalytic model systems and in situ spectroscopic and microscopic techniques for applications in energy and environmental engineering. Colloid nanoparticle synthesis provides new opportunities to tune catalytic activity and selectivity via synthetic control of the size, composition, and shape of nanoparticles. Metal–oxide interfaces are catalytically active, suggesting the tunability of catalytic activity via engineering of metal–oxide interfaces. Energy conversion from photon or chemical energy to electrical energy has been studied via utilization of hot electron flows with metal–semiconductor nanodiodes. New in situ microscopic and spectroscopic techniques have been developed to uncover the atomic structure, mobility, reaction intermediates, and oxidation states that determine catalytic activity and selectivity. Breakthroughs in these research topics can help in the smart design of catalytic and energy materials with better performance and lower cost and may lead to new methods for renewable energy conversion.

J.Y. Park (✉)

Graduate School of EEWS (WCU) and NanoCentury KI, Korea Advanced Institute of Science and Technology (KAIST), Daejeon, Republic of Korea

Center for Nanomaterials and Chemical Reactions, Institute for Basic Science, Daejeon 305-701, South Korea
e-mail: jeongypark@kaist.ac.kr

G.A. Somorjai

Department of Chemistry, University of California, Berkeley, CA 94720, USA

1.2 Materials and Pressure Gaps

The materials and pressure gaps have been a long-standing challenge in the field of heterogeneous catalysis and have transformed surface science and biointerfacial research. In heterogeneous catalysis, the materials gap refers to the discontinuity between well-characterized model systems and industrially relevant catalysts [1–6]. While the majority of surface science studies have been carried out on well-defined single crystal surfaces under ultrahigh vacuum (UHV) conditions, most catalytically active systems are employed at high pressure or at solid–liquid interfaces; this gap between UHV and industrial conditions is known as the pressure gap. The materials and pressure gaps are illustrated in Fig. 1.1. Single crystal metal surfaces have been useful model systems to elucidate the role of surface defects and the mobility of reaction intermediates in catalytic reactivity and selectivity [7, 8]. Surface scientists have been able to uncover many of the key aspects of heterogeneous catalysis by using metal single crystals as model catalyst systems. Despite the presence of defects, such as steps and kinks, single crystals are the simplest model catalysts due to the repetition of the same surface structure on terraces across the sample, as shown in Fig. 1.1. Their large size and high electrical conductivity allow their use in both photon- and electron-based surface science techniques and permit the study of low turnover (number of product molecules per site per second) catalytic reactions. These well-defined crystals allow for correlation of the surface structure with molecular adsorption and catalytic turnover by use of surface sensitive techniques, such as low energy electron diffraction (LEED), X-ray photoelectron spectroscopy (XPS), scanning tunneling microscopy (STM), and sum frequency generation (SFG) vibration spectroscopy.

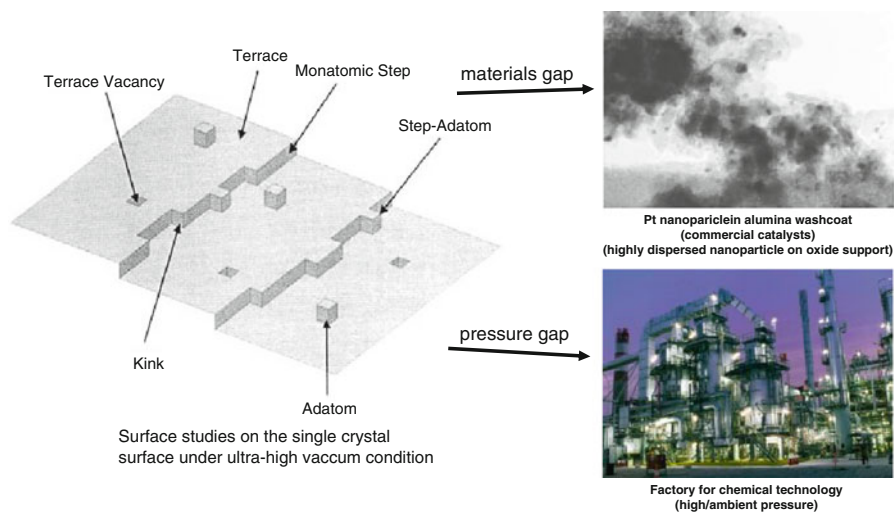


Fig. 1.1 Illustration depicting materials and pressure gaps

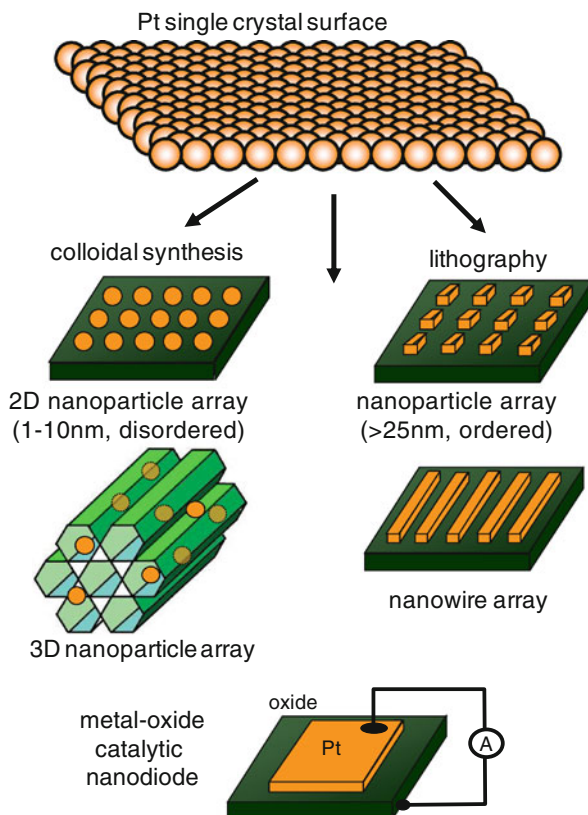


Fig. 1.2 Schematic showing the evolution of the catalyst model system from a single crystal metal surface to 2D and 3D nanoparticle arrays that are colloid synthesized and to nanowire arrays and nanodiodes that are fabricated using lithography. (Adapted from ref [5], reprinted with permission)

The use of single crystals as model catalytic systems has shed light on many surface phenomena, which, in turn, has helped to choose metallic clusters for use in industrial catalysis. Industrial catalysts, however, do not just consist of metal, but are made up of metal particles in the 1–100 nm size regime dispersed in a high surface area support. They are produced by synthesizing the metal particles and support separately and then dispersing the metal clusters onto the support using various techniques (e.g., wet-impregnation, co-precipitation, or ion-exchange). Thus, the single-crystalline metals used for modeling industrial catalysis inherently lack the complexity needed to uncover many of the factors important to catalytic turnover and selectivity. Considerations, such as metal support interactions and the importance of metallic cluster size, are of extreme importance to catalytic applications. This demand has driven development of new catalytic model systems. Figure 1.2 shows the evolution of catalytic model systems from the single crystal

surface to more complex Pt nanostructure arrays and catalytic nanodiode schemes that aid in determining the role of size, shape, composition, oxidation states, and metal–oxide interfaces in catalytic activity and selectivity. This book will outline recent work on surface science studies of single crystals and nanoparticles in Parts I and II.

In order to transition from single crystal studies to more industrially relevant catalysts, two-dimensional (2D) or three-dimensional (3D) cluster arrays are useful because the instrumentation developed for single crystal studies can also apply [9]. Recently, many different methods have been used to prepare different types of 2D model catalysts, such as spin-casting of metal salt solutions onto planar oxide supports followed by calcination, evaporation of metal films onto oxide supports, plasma deposition, laser interference nanolithography, colloidal lithography, and photolithography. All of these methods have problems that limit their applicability to industrial catalysis. Non-lithographic methods are able to access the sub-100 nm size regime interesting for catalytic applications, but are unable to exert the control necessary to uncover any dependence on metallic cluster size and shape. The goal in 2D model catalyst development is to synthesize well-characterized and reproducible catalysts in the 1–30 nm range, where the high surface area properties of the catalysts are most pronounced, as described below.

1.3 Size, Shape, and Compositional Control of Colloid Nanoparticles

In colloidal synthesis, nanoparticles are the product of the reduction of metallic salts in solution. Chemical reduction methods, including alcohol reduction, hydrogen reduction, and sodium borohydride reduction, were reported. Capping agents, such as polymers, dendrimers, block copolymer micelles, and surfactants, are used for stabilizing the nanoparticles and preventing aggregation. By using hexachloroplatinic acid or rhodium acetyl acetonate as precursor monomers, it is possible to produce monodispersed metal nanoparticles where each is coated with a polymer layer that prevents aggregation in solution (Fig. 1.3). Under optimized reduction conditions, it is possible to control the size and shape of the platinum or rhodium nanoparticles. Figure 1.4 shows platinum nanoparticles with controlled size and shape [9–13]. High-resolution transmission electron microscopy (HRTEM) reveals the shape of the nanoparticles. In the case of Pt/Rh bimetallic nanoparticles under well-defined conditions, the particle size is proportional to the monomer concentration and can be controlled by changing the monomer concentration [14].

A 2D assembly of colloid nanoparticles was developed as a new model catalyst. The Pt nanoparticles were immobilized onto the native oxide layer of a Si wafer via Langmuir-Blodgett (LB) deposition, forming a monolayer of monodispersed Pt nanoparticles, as shown in Fig. 1.5. The average interparticle spacing can be tuned by varying the surface pressure in the LB film. This approach has the advantage of controlling the size and shape of the nanoparticles; an oxide–metal interface also

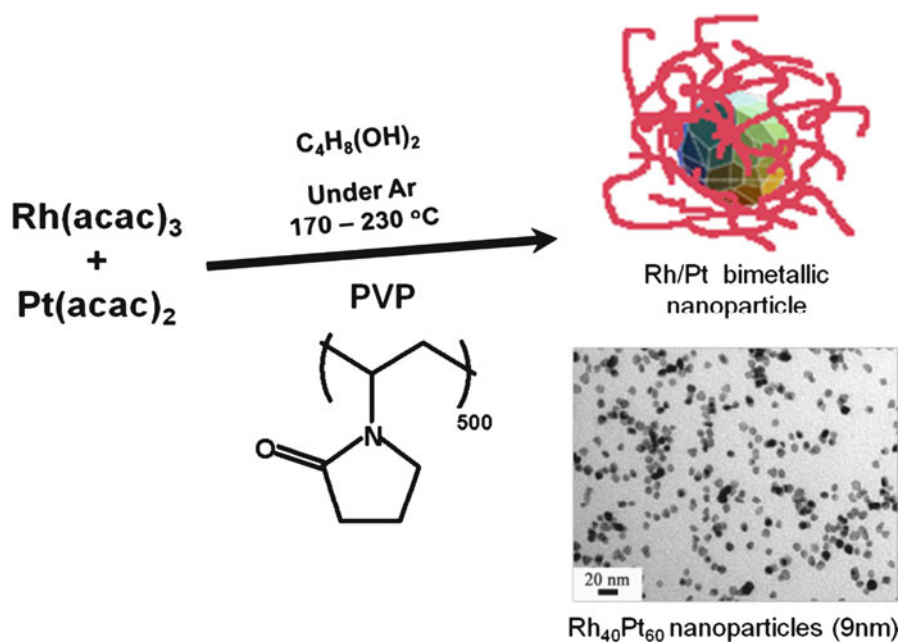


Fig. 1.3 Scheme showing the one-step synthesis of monodispersed Rh/Pt bimetallic nanoparticles [(acac) acetyl acetonate]. (Adapted from ref [28], reprinted with permission)

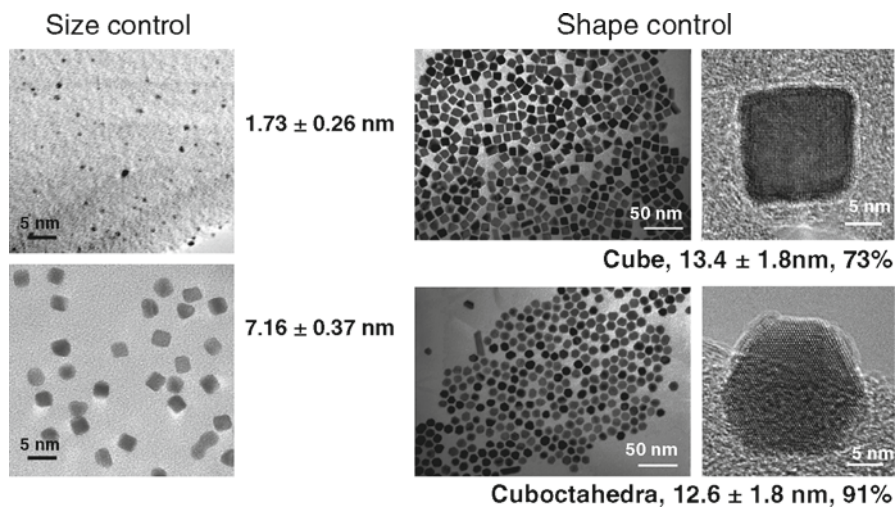


Fig. 1.4 Size and shape control of Pt colloid nanoparticles. Monodispersed platinum nanoparticles 1.7 and 7.2 nm in size (*left*) with well-controlled cubic or cuboctahedral shapes (*right*). Scale bar: (*left*) 5 nm, (*center*) 50 nm, and (*right*) 5 nm. The % values (*right*) refer to the % of nanoparticles with the corresponding shape. (Adapted from ref [28], reprinted with permission)

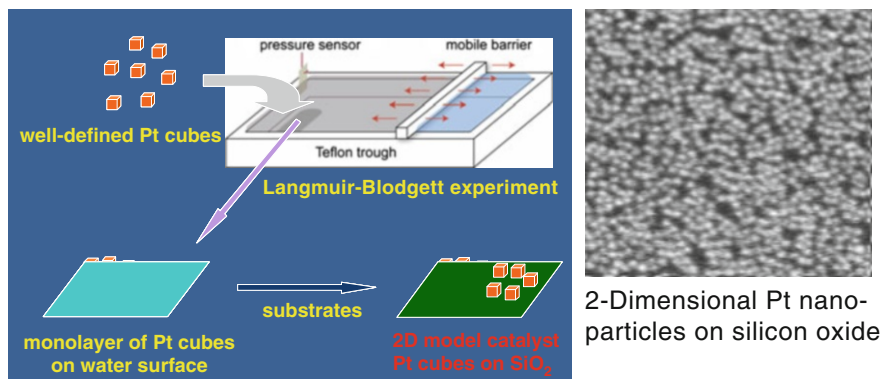


Fig. 1.5 Schematic of the Langmuir-Blodgett method and TEM image of 2D Pt nanoparticle arrays on a silicon oxide surface fabricated using the Langmuir-Blodgett method

forms between the nanoparticles and substrate when using colloidal synthesis. The bond configuration, structural, compositional, and electronic structures of 2D assemblies of colloid nanoparticles can be characterized using surface-sensitive techniques, including scanning probe microscopy, X-ray photoelectron spectroscopy, and SFG vibration spectroscopy.

1.4 Control of Catalytic Reactions via Tuning the Size and Composition of Bimetallic Nanoparticles

Composition is another important factor that influences catalytic activity and selectivity. Pt/Rh bimetallic nanoparticles with variable composition and constant size (9 nm) were synthesized using a one-pot polyol synthetic method [14]. The activity of CO oxidation on these bimetallic nanoparticles was studied. Colloid techniques use chloroplatinic acid or a rhodium precursor (like rhodium acetylacetonate) in the presence of a polymer (PVP) to make metal ions. These metal ions are then reduced in alcohol. Figure 1.6a shows XPS spectra measured on 2D Rh_xPt_{1-x} ($x=0-1$) nanoparticle arrays on a silicon surface. The intensity of the Rh3d peak increases, while the Pt4f and Pt4d peaks decrease as the composition of Rh increases. Figure 1.6b shows TEM images of monodispersed Rh_{0.4}Pt_{0.6} nanoparticles. The particles were 9.3 ± 1.2 nm in size, which was determined by measuring 150 nanocrystals from a TEM image. Once monodispersed particles with the desired size and composition are obtained, we put them in a Langmuir trough and apply a certain surface pressure to deposit different densities of nanoparticle monolayer films. The turnover rate of a pure Rh nanoparticle is 20 times that of a Pt nanoparticle under the reaction conditions used (100 Torr O₂, 40 Torr CO at 180 °C). Rh_xPt_{1-x} ($x=0.2-0.8$) particles exhibit an intermediate activity, as shown in Fig. 1.6c, while the activation energy increases from 25 to 27 kcal mol⁻¹ with increasing rhodium content.

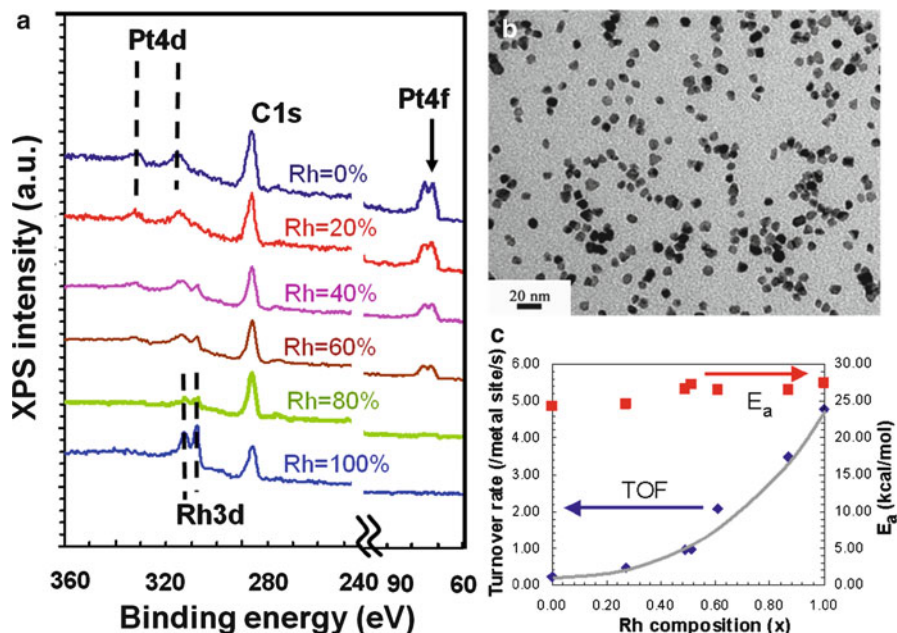
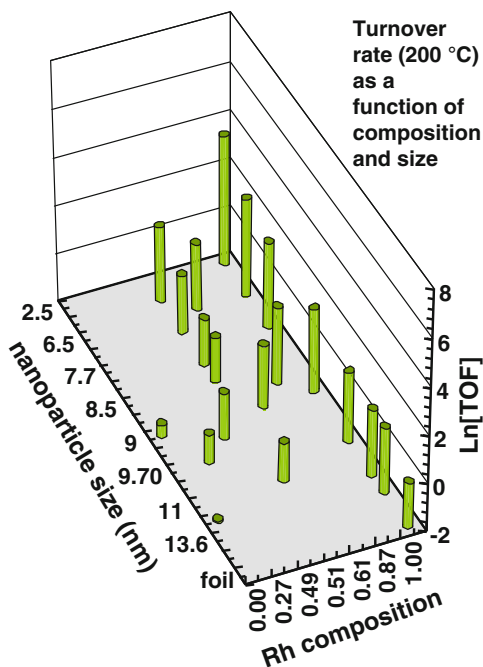


Fig. 1.6 (a) The XPS plots measured on two-dimensional Rh_xPt_{1-x} ($x=0-1$) nanoparticle arrays on a silicon surface. (b) TEM images of the Rh_{0.4}Pt_{0.6} nanoparticles. (c) Plot of the turnover frequency (TOF) of Rh_xPt_{1-x} measured at 180 and 200 °C, and the activation energies of nanoparticle arrays as a function of Rh composition ($x=0-1$). (Adapted from ref [14], reprinted with permission)

The observation that pure Rh nanoparticles are more reactive than Pt nanoparticles is consistent with earlier CO oxidation studies on thin films and single crystals. This is associated with differences in the initial dissociative sticking probability of oxygen (Pt is 0.2 and Rh is 1.0). As shown in Fig. 1.6c, the reactivity of CO oxidation increases nonlinearly as a function of Rh composition. This tendency could be due to preferential migration of Pt to the surface, resulting in a higher surface concentration of Pt compared to the bulk concentration. The size of the Rh_{0.5}Pt_{0.5} bimetallic nanoparticle arrays can be used to tune the activity of CO oxidation. The size was varied during synthesis using colloidal chemistry. The catalytic activity of CO oxidation increases as the size of the bimetallic nanoparticles decreases. Thermodynamic analysis and XPS measurements suggest that the higher catalytic activity of smaller bimetallic nanoparticles is associated with the preferential surface segregation of Rh, compared to Pt, on the smaller nanoparticles [15]. Figure 1.7 shows the turnover rate of CO oxidation measured on Rh/Pt nanoparticles as a function of size and composition. The general trend of the size and compositional dependence on catalytic activity is that the smaller and Rh-rich nanoparticles exhibit higher catalytic activities. This result suggests the intriguing capability of changing the catalytic activity in a bimetallic nanoparticle by varying the composition and size, with possible applications in tunable nanocatalysts [16, 17].

Fig. 1.7 Turnover rate of CO oxidation measured on Rh/Pt nanoparticles as a function of size and composition



1.5 In Situ Surface Characterization to Bridge Pressure Gaps

Vacuum studies on single crystal surfaces revealed a number of important surface phenomena, leading to new concepts in surface science. The instrumentation techniques developed for surface studies include photon-in/electron-out (XPS), electron-in/electron-out (LEED surface crystallography and Auger electron spectroscopy (AES)), atomic, molecular beams, and ion beam in/ions out (secondary ion mass spectrometry (SIMS), and inelastic ion surface scattering (ISS)) techniques. All of these techniques have high scattering cross sections that would not survive the presence of high-pressure gas or liquid at the interfaces.

Since the 1980s, the surface science community has developed techniques that probe the structure, composition, mechanical properties, and dynamics of surfaces at high pressure. The research activity on in situ surface characterization will be covered in Part III. Several examples of high-pressure surface apparatuses are shown in Fig. 1.8. These include (a) high-pressure SFG vibration spectroscopy, (b) high-pressure STM, (c) high-pressure XPS, and (d) atomic force microscopy (AFM).

Of these, SFG vibrational spectroscopy is a surface-specific technique; it is quite useful for high-pressure studies based on the principle of second harmonic generation (see Fig. 1.8a). One or both laser frequencies are tuned, then spatially and temporally overlapped. By scanning one of the lasers in the infrared frequency

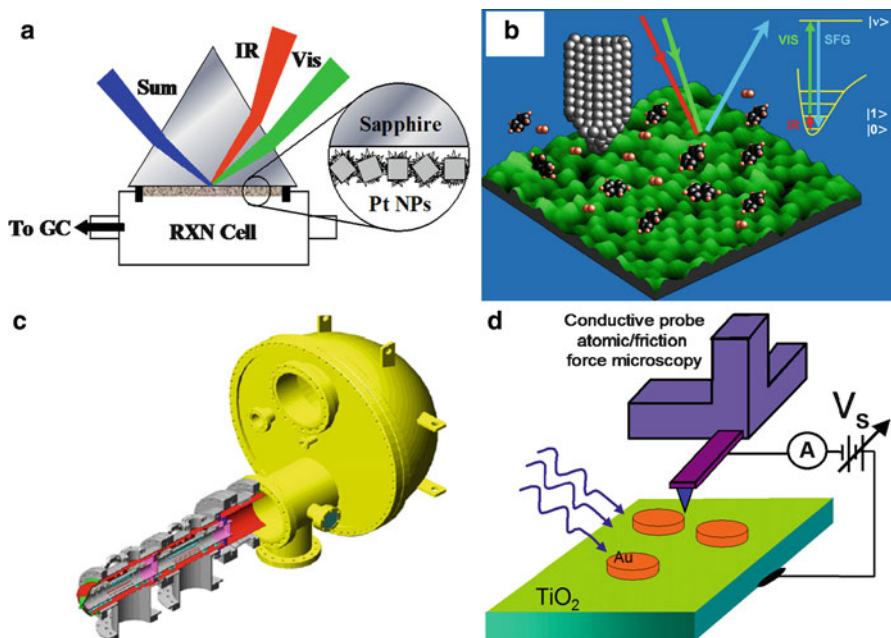


Fig. 1.8 Schemes of high-pressure surface apparatuses: (a) high-pressure sum frequency generation (SFG) vibration spectroscopy, (b) high-pressure STM, (c) ambient pressure XPS, and (d) in situ AFM. (Adapted from ref. [28], reprinted with permission)

regime, a sum frequency signal and, thus, a visible vibrational spectrum is obtained [7]. Such a signal is forbidden from a centrosymmetric medium, such as in the bulk of face-centered cubic crystals or in an isotropic high-pressure gas or a liquid. However, at a surface, which is not centrosymmetric, the second-order susceptibility is non-zero, and the surface yields a vibrational spectrum with monolayer sensitivity. It is also able to give vibrational frequencies of adsorbed molecules at pressures ranging through 10–12 orders of magnitude. High-pressure STM images (shown in Fig. 1.8b) reveal that at high pressure, surfaces form new structures that are not seen under ultrahigh vacuum. As more molecules adsorb onto the surface, the repulsive interaction among them becomes more important and causes the surface to reconstruct in new ways.

Using high-pressure STM, we always find that the adsorbed layer is mobile on the catalytically active surface, while ordered structures form if the reaction is inhibited by another adsorbate that poisons the catalytic reaction [18]. Catalytic hydrogen/deuterium exchange on a platinum (111) single crystal and its poisoning with carbon monoxide was also studied using STM and mass spectrometry at pressures ranging from mTorr to atmospheric. STM images acquired at room temperature under reaction conditions (200 mTorr H₂, 20 mTorr D₂) show a surface with no discernible order (Fig. 1.9a), as the adsorbate species diffuse much faster than the scanning rate of the instrument (10 nm per millisecond) [19]. However, after

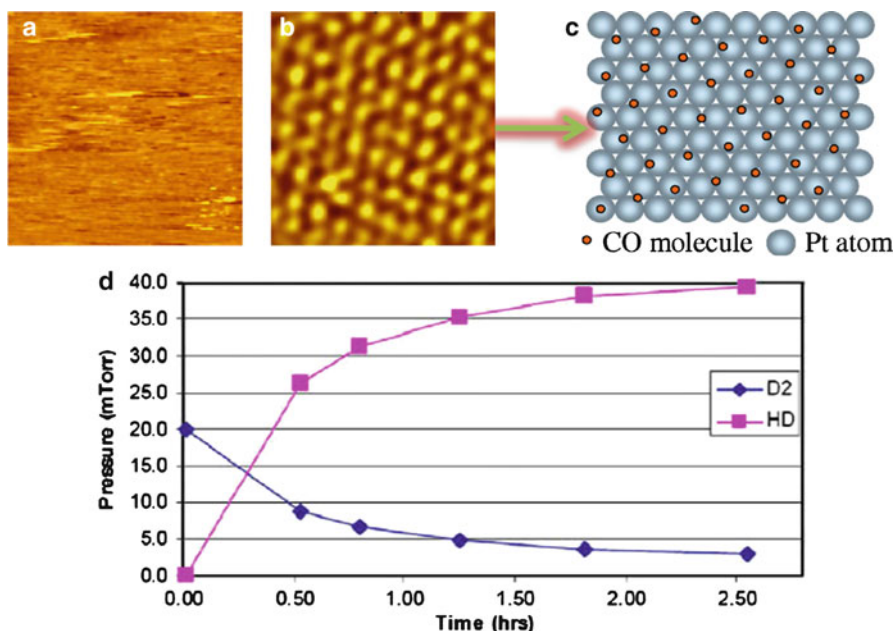


Fig. 1.9 High-pressure STM results. $90 \text{ \AA} \times 90 \text{ \AA}$ STM images of catalytically active Pt(111) at 298 K in the presence of (a) 200 mTorr H₂ and 20 mTorr D₂ and (b) 200 mTorr H₂, 20 mTorr D₂, and 5 mTorr CO. (c) CO molecules are represented by the small circles and color coded according to their proximity to a top site (*dark*) or to a bridge site (*light*). (d) D₂ and HD at 296 K, 200 mTorr H₂, and 20 mTorr D₂ were monitored using mass spectroscopy. The evolution of the D₂ and HD partial pressures indicates that the Pt catalyst surface is actively producing HD, consistent with the STM image (a). (Adapted from ref. [18], reprinted with permission)

introducing 5 mTorr of CO to poison the reaction, STM images reveal an ordered surface with hexagonal symmetry (Fig. 1.9b), which is similar to that formed by pure CO on Pt(111) in this pressure range. The structure is incommensurate with that of the Pt(111) lattice and has a coverage of about 0.6 monolayer. A schematic of the proposed structure is shown in Fig. 1.9c. At room temperature and in the presence of 200 mTorr H₂ and 20 mTorr D₂, the surface is catalytically active, producing HD at a rate of 4.3 molecules/site/s, as shown in Fig. 1.5d. Upon introduction of 5 mTorr of CO, however, the production of HD dropped below the detection limit of our mass spectrometer. At 345 K, the turnover frequency in the absence of CO increased to 39 molecules/site/s, which is about ten times higher than at room temperature. The addition of 5 mTorr of CO at this temperature dramatically decreased the reactivity, but unlike in the room temperature case, the catalytic activity was still observed at 0.03 molecules/site/s. This implies that the immobile, ordered monolayer of CO molecules forms an incommensurate structure relative to the Pt(111) substrate. Removing a small fraction of the CO layer by heating the sample allowed the surface to become mobile and catalytically active.

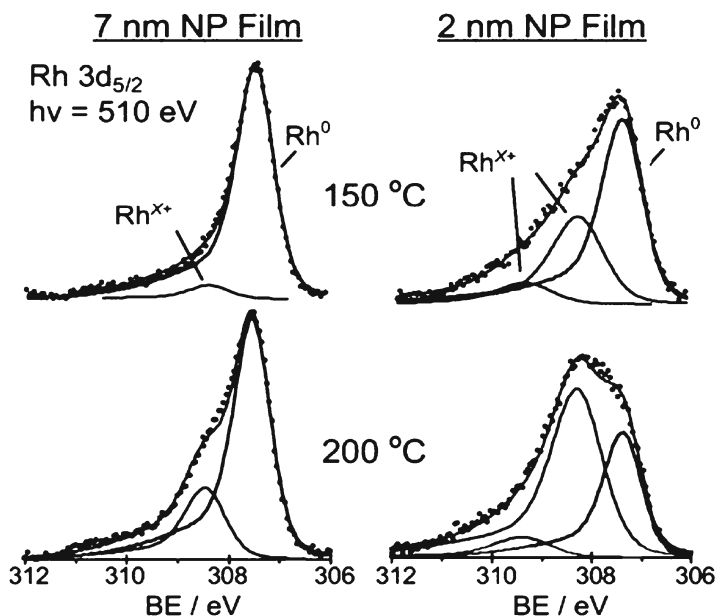


Fig. 1.10 XPS Rh3d peaks for 2 and 7 nm Rh nanoparticle arrays during CO oxidation taken with ambient pressure XPS. (Adapted from ref [10], reprinted with permission)

The surface composition and oxidation of single crystals or nanoparticles under gas or catalytic conditions can be studied by using ambient pressure X-ray photoelectron spectroscopy (AP-XPS) [20, 21]. A schematic representation of AP-XPS is shown in Fig. 1.8c, which illustrates a differentially pumped electrostatic lens system that refocuses the scattered electrons into the object plane of a standard electron energy analyzer in the high-vacuum region. The kinetic energy of the detected electrons can be varied by tuning the photon energy of the X-ray source. Figure 1.10 shows XPS Rh3d peaks for 2 and 7 nm Rh nanoparticle arrays during CO oxidation taken with ambient pressure XPS. The high catalytic activity of the smaller Rh nanoparticles is associated with the presence of Rh oxide, suggesting the intrinsic role of Rh oxide as a catalytically active species [10].

AFM is a technique whereby a small tip (tens of nm) is raster scanned across a surface. A laser light is reflected off of the back of the tip, and the reflected light is collected in a position-sensitive photodiode. This allows for gathering such information as surface topography and for measuring mechanical properties of the surface, such as friction, adhesion, stiffness, and plastic deformation. The friction and adhesion properties of colloid nanoparticles were investigated using AFM [22]. Figure 1.11 shows AFM images of Pt colloid nanoparticles with four types of capping layers: TTAB (tetradecyltrimethylammonium bromide), HDA (hexadecylamine), HDT (hexadecylthiol), and PVP (poly(vinylpyrrolidone)). The variation of friction when changing the capping layers is approximately 30 %; it appears that the friction depends on the packing and ordering of the capping layers.

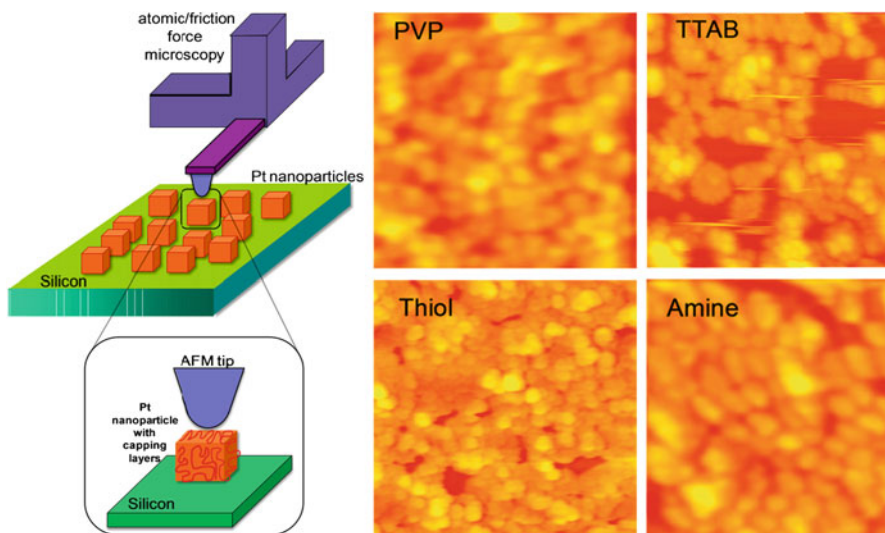


Fig. 1.11 (Left) Scheme of AFM on Pt nanoparticles. (Right) AFM images (500×500 nm) of Pt nanoparticles capped with various capping layers. (Adapted from ref. [22], reprinted with permission)

1.6 The Role of Metal–Oxide Interfaces in Heterogeneous Catalysis

One of the key issues in heterogeneous catalysis is the role of metal–oxide interfaces in altering catalytic activity. The smart design of nanocatalysts can improve the catalytic activity of transition metals on reducible oxide supports, such as Pt nanoparticles or nanowires on a titania substrate, as shown in Fig. 1.12, via strong metal–support interactions (SMSI). The SMSI effect refers to changes in the catalytic activity when group VIII metals (i.e., Fe, Ni, Rh, Pt, Pd, and Ir) are supported on certain oxides (e.g., TiO_2 , TaO_5 , CeO_2 , NbO). For example, methane formation from CO or CO_2 and H_2 is enhanced by three orders of magnitude.

The role of the metal–oxide interface in enhancing catalytic activity was first suggested by Schwab and others, who performed oxidation of carbon monoxide on Ag/NiO. As reported by Hayek and others, the reaction rate in the oxide–metal model system depends on the oxidation state of the supporting oxide, the free metal surface area, and the number of sites at the interface between the metal and the support. The origin of such metal–oxide interactions is attributed to either geometric or electronic effects. The geometric effect assumes that the active surface area of the noble metal changes during the reduction process.

The electronic effect involves charge transfer between the metal and the oxide support. Elucidation of the origin of the metal–support interaction requires measurement of the charge transfer through the oxide–metal interface. To detect this

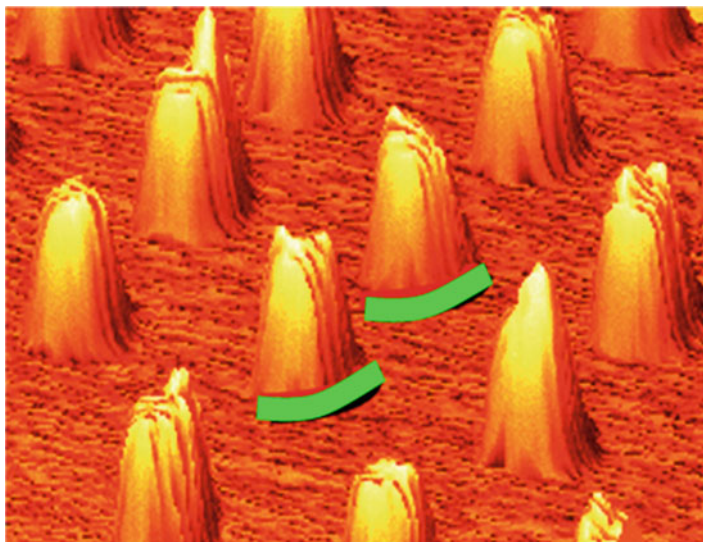


Fig. 1.12 AFM image of Pt nanoparticles on silicon oxide

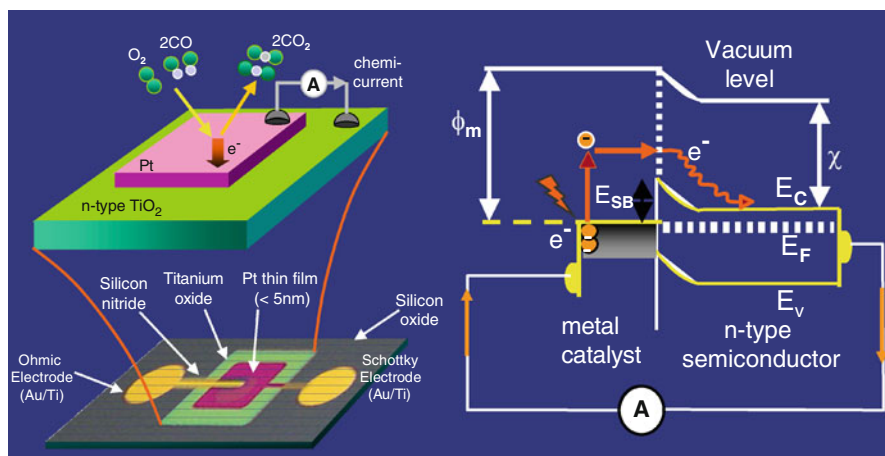


Fig. 1.13 (left) Scheme of catalytic nanodiodes and (right) energy diagram of catalytic nanodiodes

charge transfer or flow of hot electrons under catalytic reaction conditions, metal–semiconductor Schottky diodes have been developed [23, 24]. If the metal particle or film is the diameter or thickness of the electron mean-free path ($\sim 10\text{ nm}$), hot electrons can be collected as they are transported across the metal without collision, as shown in Fig. 1.13. For an n-type Schottky diode, hot electrons are detected as a chemi-current if their excess energy $E_{\text{ex}} = |E - E_F|$ is larger than the effective Schottky barrier, which is the difference between the conduction band minimum and the

Fermi energy, E_F , at the interface. Once hot electrons arrive at the oxide, they dissipate energy and thus cannot go back to the metal. Therefore, the Schottky energy barrier leads to irreversible, one-way charge transfer of hot electrons from the metal to the semiconductor, as shown in Fig. 1.13. After hot electrons move from the metal to the semiconductor, they are replaced by low-energy electrons supplied by the external leads connected to the Pt and the semiconductor, resulting in the continuous flow of hot electrons generated by the catalytic reaction.

The hot electron flows also correlate with the turnover rate of CO oxidation, as measured separately by gas chromatography [25]. Photon energy has been observed being converted into hot electron flows with metal–semiconductor diodes [26, 27]. The detection of hot electrons may lead to a fundamental understanding of energy dissipation and conversion processes, which would introduce new opportunities for energy conversion. The detection of hot electrons under various catalytic reactions and the influence of hot electrons in catalytic reactivity will be discussed in Chap. 10.

1.7 Conclusion

This chapter outlines new research directions in surface science and their relationship to nanocatalysts and renewable energy conversion. We envision three subjects which are important research directions: (1) development of new model systems and functional materials for applications in energy and the environment, (2) in situ surface characterization to reveal surface phenomena under conditions where catalytic processes or energy conversion commonly take place, and (3) new device schemes for energy conversion. Due to advancements in these research areas, surface science is entering a new era and will become an area of research essential to truly achieving renewable energy sources, which is an important goal for mankind.

References

1. Somorjai GA, Li Y (2010) Introduction to surface chemistry and catalysis. Wiley, New York
2. Ertl G, Knözinger H, Schüth F, Weitkamp J (2008) Handbook of heterogeneous catalysis, vol 8. Wiley, New York
3. Ertl G, Freund HJ (1999) Catalysis and surface science. *Phys Today* 52:32–38
4. Freund HJ et al (2001) Bridging the pressure and materials gaps between catalysis and surface science: clean and modified oxide surfaces. *Top Catal* 15:201–209
5. Somorjai GA, York RL, Butcher D, Park JY (2007) The evolution of model catalytic systems; studies of structure, bonding and dynamics from single crystal metal surfaces to nanoparticles, and from low pressure (10^{-3} torr) to high pressure (>math>10^{-3}</math> torr) to liquid interfaces. *Phys Chem Chem Phys* 9:3500–3513. doi:[10.1039/b618805b](https://doi.org/10.1039/b618805b)
6. Somorjai GA, Park JY (2008) Molecular surface chemistry by metal single crystals and nanoparticles from vacuum to high pressure. *Chem Soc Rev* 37:2155–2162. doi:[10.1039/b719148k](https://doi.org/10.1039/b719148k)
7. Somorjai GA, Park JY (2007) Frontiers of surface science. *Phys Today* 60:48–53

8. Campbell CT (1997) Ultrathin metal films and particles on oxide surfaces: structural, electronic and chemisorptive properties. *Surf Sci Rep* 27:1–111
9. Song H, Kim F, Connor S, Somorjai GA, Yang PD (2005) Pt nanocrystals: shape control and langmuir-blodgett monolayer formation. *J Phys Chem B* 109:188–193
10. Grass ME et al (2008) A reactive oxide overlayer on rhodium nanoparticles during CO oxidation and its size dependence studied by in situ ambient-pressure X-ray photoelectron spectroscopy. *Angew Chem Int Ed* 47:8893–8896. doi:[10.1002/anie.200803574](https://doi.org/10.1002/anie.200803574)
11. Zhang Y et al (2007) One-step polyol synthesis and langmuir-blodgett monolayer formation of size-tunable monodisperse rhodium nanocrystals with catalytically active (111) surface structures. *J Phys Chem C* 111:12243–12253
12. Lee H et al (2006) Morphological control of catalytically active platinum nanocrystals. *Angew Chem Int Ed* 45:7824–7828
13. Joo SH et al (2010) Size effect of ruthenium nanoparticles in catalytic carbon monoxide oxidation. *Nano Lett* 10:2709–2713. doi:[10.1021/nl101700j](https://doi.org/10.1021/nl101700j)
14. Park JY, Zhang Y, Grass M, Zhang T, Somorjai GA (2008) Tuning of catalytic CO oxidation by changing composition of Rh-Pt bimetallic nanoparticles. *Nano Lett* 8:673–677. doi:[10.1021/nl073195i](https://doi.org/10.1021/nl073195i)
15. Park JY, Zhang Y, Joo SH, Jung Y, Somorjai GA (2012) Size effect of RhPt bimetallic nanoparticles in catalytic activity of CO oxidation: role of surface segregation. *Catal Today* 181:133–137. doi:[10.1016/j.cattod.2011.05.031](https://doi.org/10.1016/j.cattod.2011.05.031)
16. Somorjai GA, Park JY (2008) Colloid science of metal nanoparticle catalysts in 2D and 3D structures. Challenges of nucleation, growth, composition, particle shape, size control and their influence on activity and selectivity. *Top Catal* 49:126–135. doi:[10.1007/s11244-008-9077-0](https://doi.org/10.1007/s11244-008-9077-0)
17. Norskov JK, Bligaard T, Rossmeisl J, Christensen CH (2009) Towards the computational design of solid catalysts. *Nat Chem* 1:37–46. doi:[10.1038/nchem.121](https://doi.org/10.1038/nchem.121)
18. Somorjai GA, Park JY (2009) Concepts, instruments, and model systems that enabled the rapid evolution of surface science. *Surf Sci* 603:1293–1300. doi:[10.1016/j.susc.2008.08.030](https://doi.org/10.1016/j.susc.2008.08.030)
19. Montano M, Bratlie K, Salmeron M, Somorjai GA (2006) Hydrogen and deuterium exchange on Pt(111) and its poisoning by carbon monoxide studied by surface sensitive high-pressure techniques. *J Am Chem Soc* 128:13229–13234. doi:[10.1021/ja063703a](https://doi.org/10.1021/ja063703a)
20. Salmeron M, Schlögl R (2008) Ambient pressure photoelectron spectroscopy: a new tool for surface science and nanotechnology. *Surf Sci Rep* 63:169–199
21. Tao F et al (2008) Reaction-driven restructuring of Rh-Pd and Pt-Pd core-shell nanoparticles. *Science* 322:932–934. doi:[10.1126/science.1164170](https://doi.org/10.1126/science.1164170)
22. Park JY (2011) Tuning nanoscale friction on Pt nanoparticles with engineering of organic capping layer. *Langmuir* 27:2509–2513. doi:[10.1021/la104353f](https://doi.org/10.1021/la104353f)
23. Hervier A, Renzas JR, Park JY, Somorjai GA (2009) Hydrogen oxidation-driven hot electron flow detected by catalytic nanodiodes. *Nano Lett* 9:3930–3933. doi:[10.1021/nl9023275](https://doi.org/10.1021/nl9023275)
24. Nienhaus H (2002) Electronic excitations by chemical reactions on metal surfaces. *Surf Sci Rep* 45:3–78
25. Park JY, Somorjai GA (2006) The catalytic nanodiode: detecting continuous electron flow at oxide-metal interfaces generated by a gas-phase exothermic reaction. *Chemphyschem* 7:1409–1413
26. Somorjai GA, Frei H, Park JY (2009) Advancing the frontiers in nanocatalysis, biointerfaces, and renewable energy conversion by innovations of surface techniques. *J Am Chem Soc* 131:16589–16605. doi:[10.1021/ja9061954](https://doi.org/10.1021/ja9061954)
27. Lee YK et al (2011) Surface plasmon-driven hot electron flow probed with metal–semiconductor nanodiodes. *Nano Lett* 11:4251–4255. doi:[10.1021/nl2022459](https://doi.org/10.1021/nl2022459)
28. Somorjai GA, Park JY (2008) Molecular factors of catalytic selectivity. *Angew Chem Int Ed* 47:9212–9228. doi:[10.1002/anie.200803181](https://doi.org/10.1002/anie.200803181)